Research on grouting structure design method of airport precast concrete pavement

Hongjia Zhu[1], Shitao Wu[1, 2]

[1]China Airport Planning and Design Institute Co., Ltd. Southwest Branch, Chengdu 612000, China

[2]wstxx77@163.com

Abstract. Precast concrete pavement offers significant advantages such as reduced on-site construction time and faster traffic opening, making it highly suitable for airport applications. However, the provision of a fully supportive base structure for pavement panels has long been a challenging research area. In particular, there is a lack of comprehensive investigation into the grouting structure design for these panels. In this paper, a diffusion model of cement slurry beneath the panels is derived using theoretical methods. The study focuses on analyzing the diffusion mode, calculating the diffusion distance, and proposing a feasible design approach for the grouting structure of precast concrete pavement. Our analysis demonstrates that a rectangular grouting mode is preferable, with bottom void height of the panel ranging between 5-20mm. Moreover, it is recommended to maintain grouting sections with a width not exceeding 2.5m. For each panel, grouting is ideally performed in 2-4 sections. The findings of this study contribute to enhancing the overall effectiveness and durability of precast concrete pavement systems.

Keywords: Precast Concrete Pavement; Grouting; Structure; Diffusion Model.

1. Introduction

The precast concrete pavement technology serves as an ideal and rapid method for paving. Once the curing process is complete, concrete panels are transported to the site for assembly. With immediate traffic closure, this technique grants significant value to expedite the construction and maintenance of airport pavements [1]. In the United States, two types of precast concrete pavements have been developed: jointed precast concrete pavements and prestressed precast concrete pavements [2]. Furthermore, Japan has achieved development of a precast concrete pavement capable of facilitating secondary removal functions [3].

Several technical approaches exist for precast concrete pavement, with the primary method employing mechanical measures to adjust the elevation of concrete slabs, thereby meeting flatness requirements [4]. This is followed by grouting through reserved channels within the slabs to fill any voids beneath them. Once joint slot patching is completed, the pavement assembly construction concludes. However, certain demonstration projects have revealed that a few slabs developed cracks shortly after opening to traffic, primarily due to insufficient support underneath [5,6]. The grouting process significantly influences the support conditions of the slabs, making it a key factor in ensuring the quality and durability of precast concrete pavement. Consequently, extensive efforts have been

dedicated to overcoming challenges associated with PCP panel support conditions. Limitations concerning load transfer at joints, constructability, and panel support conditions have impeded the widespread adoption of precast concrete pavement [7].A precast concrete pavement with the composite base layer comprised of the concrete beam and the filling low strength materials(b-PCP) was proposed[8]. To facilitate grouting, holes with a diameter of 3-5cm should be strategically reserved on the slab, positioned approximately 0.5-0.7m from the slab's edge. Additionally, semicircular or rectangular grouting channels are to be created beneath the slab [9]. It is important, however, not to lay the grouting channels across the entire length or width of the slab, as this can result in excessive slurry leakage from the joints. During grouting, the pressurized slurry tends to seep from the slab edges. To mitigate this issue and enhance the void filling, sealant strips are commonly placed beneath the slab. Furthermore, by pre-setting sealant strips, the void under the slab can be divided into separate grouting sections. In a study conducted by Wang Qiao [10], technical requirements for leveling materials in self-leveling sand cushion were proposed, along with a determination of the optimal mix ratio to fulfill performance criteria such as self-leveling ability, early strength development, rapid hardening, and prevention of delamination.

The current engineering practice of designing grouting structures for precast slabs relies predominantly on empirical knowledge, lacking a comprehensive understanding of the grouting diffusion mechanism. Consequently, design methods for grouting structures remain ambiguous, and their applicability in engineering projects is limited. To address these shortcomings, this paper aims to establish a diffusion model for cement slurry through theoretical analysis, determine the diffusion distance of the slurry, investigate the factors influencing slurry diffusion, and propose a robust design methodology for grouting structures in cement precast concrete pavement. The findings presented herein serve as valuable references for the design and construction of precast concrete pavements.

2. Cement Slurry Diffusion Model

Ordinary cement slurry or mud is a suspension consisting of solid particulate materials, exhibiting characteristics of a Bingham fluid. Within Bingham fluids, the dispersed particles in the continuous phase form a cohesive network structure due to strong interparticle interactions. To initiate flow in the Bingham fluid, the network structure must be disrupted by applying a shear stress that exceeds the yield value. This shear stress has a linear relationship with the deformation rate. The constitutive equation for a Bingham fluid is represented by equation (1).

$$\tau = \eta \frac{du}{dy} + \tau_0 \tag{1}$$

where: τ is the shear stress; τ_0 is the shear yield strength of the slurry; η is the plastic viscosity of the slurry; u is the flow velocity; y is the distribution distance of slurry.

In Bingham fluids, motion occurs only when the shear stress surpasses the shear yield strength, causing the remaining fluid to slide akin to a solid material. Consequently, the flow of Bingham fluids typically encompasses two distinct regions: the "flow stable zone" (solid state), where no relative motion between fluid particles is observed, and the "velocity gradient zone" (liquid state), encompassing the region beyond the flow stable zone. The interface between these zones marks the point of yielding [11].

2.1. Rectangular Diffusion Equation for Fluid

Within the context of Bingham fluids, let us consider the height of the flow core region as c. By analyzing a fluid column with a length of dl for force analysis, the cross-sectional pressure can be calculated, as depicted in Figure 1. In cases where the shear stress τ of the slurry is lower than its yield shear strength τ_0, no relative flow is observed. Therefore, the height of the flow core region can be determined as $c = 2\tau_0 dl/dp$.

By considering the model axis as the axis of symmetry, let us assume the height of the fluid column as $2y$ (with $2y > c$). This fluid column comprises two distinct regions: the flow core region and the velocity gradient region. At the interface between the velocity gradient region and the flow core region,

the velocity gradient region undergoes a shear stress τ_0 in alignment with the flow direction. On the upper surface of the velocity gradient region, a shear stress τ is experienced in the opposite direction to the flow. Analysis of forces reveals:

$$-\eta \frac{du}{dy} dl = \left(y - \frac{1}{2}c\right) dp, \left(y > \frac{1}{2}c, dp < 0\right) \tag{2}$$
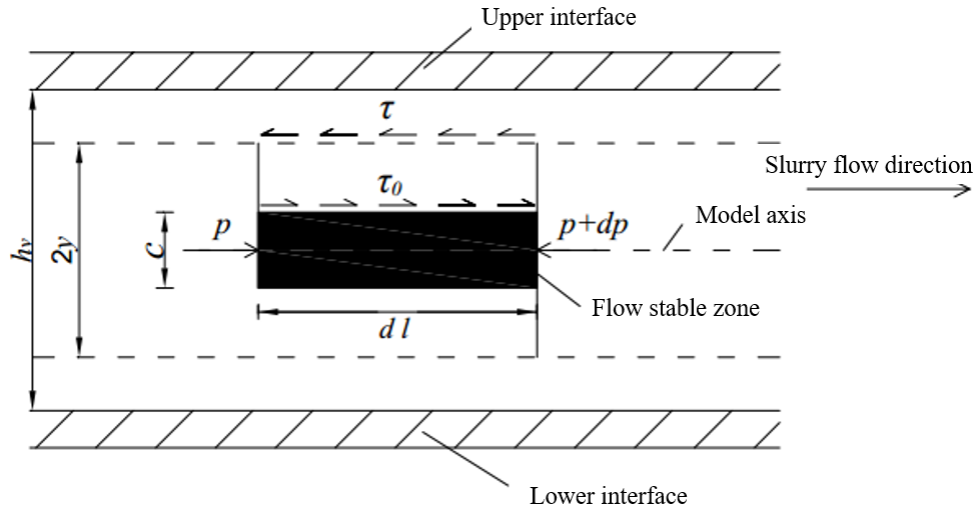
Figure 1. Slurry flow calculation diagram.

Pressure differential flow involves the generation of fluid flow solely through a pressure difference between two stationary parallel plates. The fluid viscosity causes it to remain stationary on the pipe wall. Therefore, this type of flow should satisfy certain boundary conditions: with $y = \pm\frac{h_v}{2}$, $\mu = 0$.

Upon solving differential equation (2) with $y > \frac{1}{2}c$, the resulting equation for velocity distribution constituting the cross-sectional area is as follows:

$$\mu(y) = \frac{-4y^2 J + 8\tau_0 y + h_v^2 J - 4\tau_0 h_v}{8\eta} \tag{3}$$

In the equation, J represents the hydraulic gradient, and $J = dp/dl$, h_v represents the void height between the two plates.

By considering the continuity of the velocity distribution, it is evident that the velocity remains consistent at the interface separating the velocity gradient region and the flow core region. Equation (4) provides the means to determine the velocity within the flow core region.

$$\mu\left(\frac{c}{2}\right) = \frac{\tau_0^2}{2\eta J} + \frac{J h_v^2}{8\eta} - \frac{\tau_0 h_v}{2\eta} \tag{4}$$

The velocity distribution on the cross section is as shown in Figure 2.
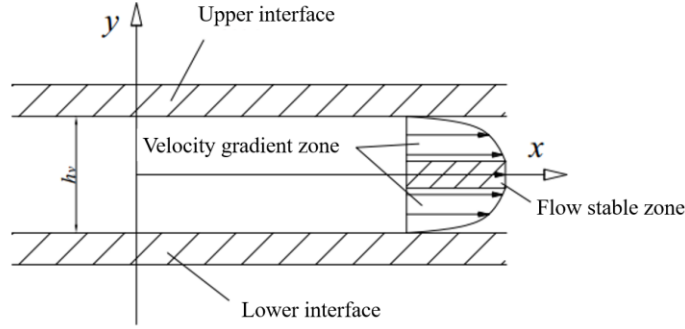
Figure 2. Slurry velocity distribution between parallel plates.

The slurry flow rate per unit width between the parallel plates can be calculated by integrating the speeds within the velocity gradient zone and the flow core zone.

$$\frac{Q}{b} = 2 \times \left[\int_0^{\frac{c}{2}} u\left(\frac{c}{2}\right) dy + \int_{\frac{c}{2}}^{\frac{h_v}{2}} u(y)dy \right] = \frac{h_v^3 J}{12\eta} + \frac{\tau_0^3}{3J^2\eta} - \frac{\tau_0 h_v^2}{4\eta} \qquad (5)$$

Where, Q represents the flow rate of the slurry, which can be considered as a constant value; the flow rate of the slurry per unit width is $q = Q/b$.

In the rectangular diffusion mode, the computational model must adhere to certain relationships regarding its dimensions. Specifically, the void height should be significantly smaller than the width of the parallel plates, while the width of the parallel plates should be much smaller than their length.
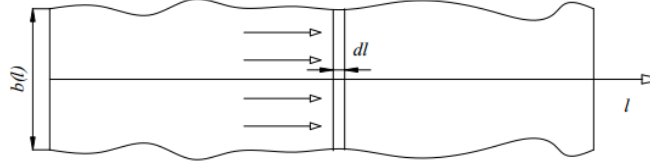
Figure 3. Slurry diffusion diagram of rectangular diffusion mode.

To facilitate ease of solution, it is prudent to simplify the aforementioned equation. When dealing with the flow of slurry, it is explicit for the height of the slurry flow core zone to remain inferior to the void height. By integrating this requirement with $c = 2\tau_0/J$, the simplified version represented as equation (6) is obtained.

$$\frac{\tau_0^3}{3J^2\eta} << \frac{h_v^3 J^3}{24J^2\eta} = \frac{h_v^3 J}{24\eta} = \frac{1}{2} \times \frac{h_v^3 J}{12\eta} \qquad (6)$$

For ease of calculation, the second term on the right-hand side of equation (5) is ignored, and the following can be obtained:

$$J = \frac{12\eta}{(h_v^3)\left(\frac{Q}{b} + \frac{\tau_0 h_v^2}{4\eta}\right)} \qquad (7)$$

For the slurry of width *dl* located at position *l* in Figure 3, the magnitude of the resistance is:

$$df = \left[2\eta \frac{du}{dy\left(\frac{h_v}{2}\right)} + \tau_0 \right] \times b(l) \times dl \qquad (8)$$

The maximum diffusion distance of the slurry is determined by the balance between the maximum injection pressure and the frictional resistance along its pathway. The diffusion process is assumed to follow a rectangular mode once the slurry is injected at the bottom of the plate. As a result, the following expression is applicable:

$$\int_0^L \left[2 \left[\eta \frac{du}{dy} \right] \left(\frac{h_v}{2} \right) + \tau_0 \right] b(l)dl = \frac{\pi}{4} \varphi^2 P \tag{9}$$

In equation (9), φ represents the diameter of the grout hole and P represents the maximum grout pressure. Based on engineering conditions, these can be considered as constant values.

For practical purposes, the width of the slurry diffusion channel is set to a constant value, denoted as b. By solving the above equation simultaneously, we can obtain the calculation formula for the maximum diffusion distance, L, of the slurry as follows:

$$L = \frac{\pi P \varphi^2 h_v^2}{48 \eta Q + 12 b h_v^2 \tau_0} \tag{10}$$

Where L is the maximum diffusion length of the slurry (m); P is the maximum grouting pressure (Pa); φ represents the diameter of the grout hole (m); h_v is the void height (m); b represents the width of the slurry diffusion channel (m); η is the plastic viscosity of the slurry ($Pa \cdot s$); τ_0 is the shear yield strength of the slurry (Pa); Q is the flow rate of the grouting machine (m³/s).

2.2. Slurry Circular Diffusion Equation

The circular diffusion model will now be solved. Figure 4 illustrates the schematic representation of the slurry diffusion.
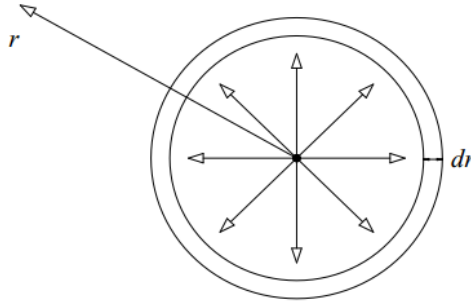
Figure 4. Slurry diffusion diagram of circular diffusion mode.

Under the provided assumption, the slurry's flow rate Q is considered constant. When the diffusion distance expands to r, the corresponding cross-section exhibits a flow rate per unit width as follows:

$$q = \frac{Q}{2\pi r} \tag{11}$$

The substitution of equation (11) into equation (5), while disregarding the second term on the right-hand side of equation (5), yields the following expression:

$$J = \frac{12\eta}{(h_v^3) \left(\frac{Q}{2\pi r} + \frac{\tau_0 h_v^2}{4\eta} \right)} \tag{12}$$

Similarly, the maximum diffusion distance of the slurry occurs when the maximum injection pressure matches the frictional resistance along the path. Assuming a circular diffusion mode after the slurry is injected at the bottom of the plate, the following expression can be derived:

$$\int_{0}^{R} \left[2 \left[\eta \frac{du}{dy} \right] \left(\frac{h_v}{2} \right) + \tau_0 \right] \times 2\pi r \, dr \; = \frac{\pi}{4} \varphi^2 P \tag{13}$$

Solving the equation yields the following expression for the circular diffusion of the slurry:

$$R = \frac{-12\eta Q + \sqrt{144\eta^2 Q^2 + 3\pi^2 \varphi^2 P \tau_0 h_v^4}}{6\pi\tau_0 h_v^2} \tag{14}$$

Where R is the maximum diffusion distance radius of the slurry (m).

3. Grouting Hole Distribution Design for Precast Pavement Panels

To achieve complete void filling with grouting slurry, it is essential to analyze the design methods for both the grouting holes and flow channels in conjunction with the slurry diffusion equations. The calculation of the slurry's plastic viscosity can be accomplished by utilizing formula (15), as provided in literature [12].

$$\eta = \eta_1 e^{\frac{K}{W}} \tag{15}$$

Where: η represents the plastic viscosity of the slurry, Pa·s; η_1 is the viscosity of water, 1×10^{-3}Pa·s; K is a constant, varying between 1.6~2.2 kg/m³ and is taken as 1.8 for calculating the plastic viscosity; W is the water-cement ratio of the slurry.

As stated in the literature [12], the shear yield strength of the slurry can be determined through the utilization of formula (16). This formula considers both the water-cement ratio and the dynamic viscosity of the slurry.

$$\tau_0 = \tau_1 e^{\frac{K}{W}} \tag{16}$$

Where: τ_0 is the shear yield strength of the slurry, Pa; $\tau_1, \tau_1 = 0.35 pa$; W is the water-cement ratio of the slurry; K is a constant, taken as 2.1.

Using standard parameters of a cement grouting machine, including a flow rate of 3 m³/h, a grouting hole diameter of 0.05 m, and a maximum pressure capability of 0.5 MPa, the width of the slurry in rectangular diffusion mode is determined to be 2.5 m. By employing a commonly used water-cement ratio of W=0.7 for ordinary cement slurry, along with a plastic viscosity of 13.09×10⁻³ Pa·s and a shear yield strength of 7.02 Pa, the maximum diffusion distance is calculated for rectangular or circular diffusion modes with varying bottom void heights (h_v), as indicated by formulas (9) and (14). The computed results are presented in Table 1.

Table 1. Slurry diffusion distance calculation.

Height of void at bottom of panel h_v (mm)	0.5	1	2	5	10	15	20	50
Rectangle diffusion length (m)	1.72	5.39	11.57	17.02	18.25	18.50	18.59	18.68
Circular diffusion radius (m)	1.58	3.00	3.62	3.82	3.85	3.85	3.86	3.86

The results presented in Table 1 demonstrate that the diffusion distance of the cement slurry increases proportionally with the size of the void at the bottom of the panel. Accordingly, the rectangular diffusion mode exhibits a larger diffusion length compared to the circular diffusion mode for voids of the same size. With a diffusion width of 2.5 m,, the maximum diffusion distance achieved in the rectangular mode for the cement slurry reaches 1.72 m, which remains greater than the 1.58 m radius in the circular diffusion mode. Consequently, the circular diffusion mode is more prone to encountering unfilled voids at the bottom of the panel. To enhance the extent of void filling with cement slurry, efforts should primarily focus on facilitating slurry diffusion in the rectangular mode.

Figure 5 illustrates the diffusion distances in the rectangular mode for slurry with varying diffusion widths b and bottom void heights h_v, while maintaining identical conditions.
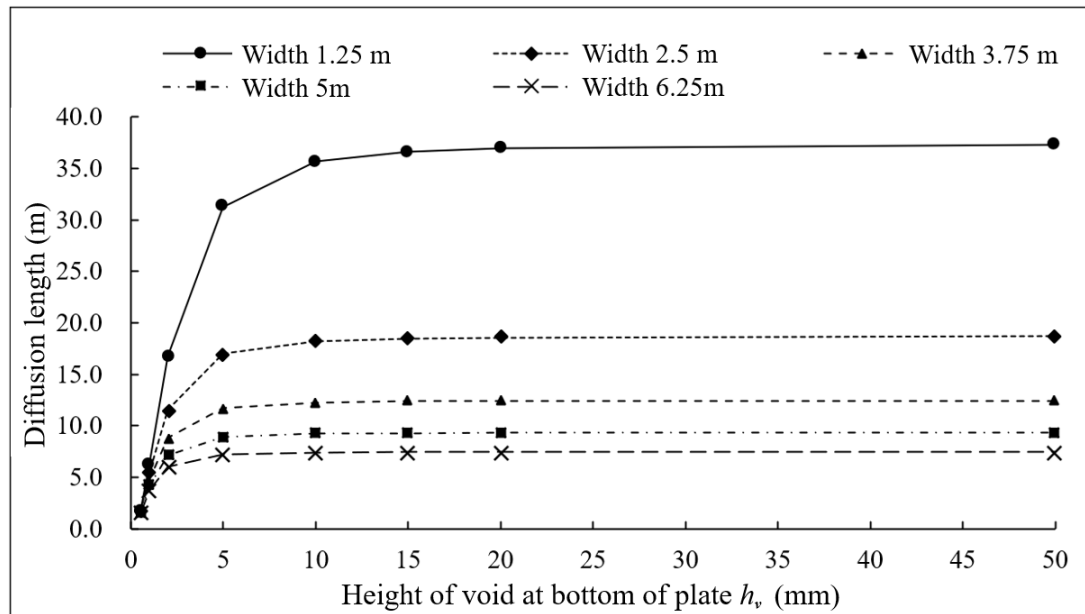
Figure 5. Different width diffusion distance of rectangular diffusion mode.

The calculated results indicate a positive correlation between the slurry diffusion length and the bottom void height of the panel. Notably, when the bottom void height is less than 5 mm, a significant and rapid increase in the diffusion distance is observed. However, within the range of 5-20 mm, the rate of increase decelerates. Beyond a void height of 20 mm, the slurry diffusion length remains essentially unchanged.

The construction of precast concrete pavement often encounters difficulties in accurately controlling the elevation of the base layer. As a result, the height of the void between the base layer and the precast panel can vary significantly. To maximize the filling of voids at the panel's bottom, it is essential to ensure that the slurry diffusion can effectively reach even the smallest 1 mm-high voids. For standard panels with a length of approximately 5 m, it is advisable to limit the diffusion width to a maximum of 2.5 m.

A reduction in the width of rectangular diffusion leads to a gradual increase in the length of slurry diffusion. Nevertheless, it is important to acknowledge that the use of smaller diffusion widths entails the need for longer work steps and construction time in practice. To minimize construction time, it is advisable to employ a diffusion width between 1.25-2.5 m. As such, for standard-sized cement concrete panels measuring 5 m × 5 m, it is recommended to divide them into 2-4 sections for separate grouting to achieve the best outcome.

Sealing material is employed to seal the bottom edges of the precast cement panels, while each section is also separated using sealing material to create a comparatively enclosed space.

In order to mitigate the potential lifting of precast cement panels caused by slurry pressure during grouting, release holes are strategically placed within the panel to facilitate the release of air from the enclosed space. Generally, these release holes are symmetrically arranged with the grouting holes and they share the same diameter, allowing for interchangeable usage in practical applications.

4. Conclusion

Grouting at the bottom of the panel is a crucial factor that significantly impacts the quality and durability of precast concrete pavement. Currently, there is insufficient research on the diffusion mechanism of grouting at the bottom of the panel, and the design methods for grouting structures remain unclear. This

deficiency hinders adequate support for engineering applications. Diffusion models for cement slurry under precast panels in rectangular and circular diffusion modes have been derived in this paper through theoretical analysis. With conventional cement grouting machines and cement slurry parameters, this study calculates the diffusion distance in rectangular and circular modes, while also analyzing the factors influencing diffusion.

The findings demonstrate that the rectangular diffusion mode outperforms the circular mode, emphasizing the preference for adopting the rectangular diffusion mode for grouting at the bottom of the panel. In the rectangular diffusion mode, the diffusion distance of cement slurry increases as the height of the void at the bottom of the panel increases. When the void at the bottom of the panel measures less than 5 mm, the diffusion distance increases relatively rapidly. However, when the void exceeds 20 mm, the diffusion distance remains essentially unchanged. Consequently, the pre-reserved void at the bottom of the panel falls within the range of 5-20 mm.

Considering the significant variability in void height between the base layer and the bottom of the panel, the width of the grout for each section should not exceed 2.5 m for conventional pavement panels. To ensure efficient construction, a section width between 1.25-2.5 m is deemed more suitable. It is advisable to divide the precast panel into 2-4 sections for separate grouting, with each section equipped with grouting holes and vent holes.

This research provides valuable guidance for the design and construction of precast concrete pavement in airports. Further research intends to investigate the diffusion distance and distribution characteristics of cement through experimental studies and subsequently enhance the design of grouting structures based on the experimental results.

References

[1] Tayabji, Shiraz, Dan Ye, and Neeraj Buch. "Precast concrete pavements: Technology overview and technical considerations." PCI journal 58.1 (2013):112-128.

[2] Tayabji, Shiraz D., Dan Ye, and Neeraj J. Buch. Precast concrete pavement technology. Transportation Research Board, 2013.

[3] Hara C, Ikeda T, Matsuno S, et al. Long-term performance of prestressed concrete pavements in Japan[C]. International Purdue Conference on Concrete Pavement Design and Materials for High Performance, 6th, Indianapolis, Indiana, USA. 1997:329-353

[4] Hara, Chisato, et al. "Long term performance of prestressed concrete pavements in Japan." International Purdue Conference on Concrete Pavement Design and Materials for High Performance, 6th, 1997, Indianapolis, Indiana, USA. Vol. 1. 1997:329-353.

[5] Syed, Ameen, and Ranjan S. Sonparote. "Development and early-age performance of an innovative prestressed precast concrete pavement." Journal of Construction Engineering and Management 146.2 (2020): 05019018.

[6] Tayabji S, Buch N, Kohler E. Precast concrete pavements: current technology and future directions[C]. 9th International Conference on Concrete Pavements. San Francisco: International Society for Concrete Pavements, 2008:17-36.

[7] Rao C, Littleton P, Sadasivam S, et al. California Demonstration Project: Pavement Replacement Using a Precast Pavement System on I-15 in Ontario[R]. Ontario: 2013.

[8] Zhao, Hongduo, et al. "Structural optimization and performance evaluation of precast concrete pavement with composite base layer." International Journal of Transportation Science and Technology 12.2 (2023): 525-533.

[9] Liu, et al. "Research and Application of Full-thickness of Cement Concrete Pavement Rapid Reparation." Journal of Highway and Transportation and Development 28.12 (2011): 525-533

[10] Wang, Qiao. "Study of rapid repair technology for precasted assembling slab of cement concrete pavement." Journal of Transport Science 2007, 23(04):33-38.

[11] Cai Shenghua.grouting method (China Embankment Engineering Construction Series 11). China Water & Power Press, 2006.

[12] Sun Zhao.dam bedrock grouting. China Water & Power Press, 2004.44